

# High pressure behavior of titanium–silicon carbide ( $\text{Ti}_3\text{SiC}_2$ )

J. L. Jordan

*School of Materials Science and Engineering, Georgia Institute of Technology, Atlanta, Georgia 30332-0245*

T. Sekine, T. Kobayashi, and X. Li

*Advanced Materials Laboratory, National Institute for Materials Science, Tsukuba 305-0044, Japan*

N. N. Thadhani<sup>a)</sup>

*School of Materials Science and Engineering, Georgia Institute of Technology, Atlanta, Georgia 30332-0245*

T. El-Raghy

*3-ONE-2 LLC, 3600 Market Street, Suite 100, Philadelphia, Pennsylvania 19104*

M. W. Barsoum

*Department of Materials Engineering, Drexel University, Philadelphia, Pennsylvania 19104*

(Received 17 January 2003; accepted 18 March 2003)

The dynamic high-pressure behavior and phase stability of titanium–silicon carbide ( $\text{Ti}_3\text{SiC}_2$ ), a unique ceramic having metal-like properties, was investigated in this study. Time-resolved measurements of the Hugoniot equation of state, employing a plate impact geometry, were conducted on the  $\text{Ti}_3\text{SiC}_2$  samples in the pressure range of 50–120 GPa using a two stage light gas gun. At pressures around 90–120 GPa,  $\text{Ti}_3\text{SiC}_2$  was found to transform to a more compressed state. Shock-recovery experiments were also performed on  $\text{Ti}_3\text{SiC}_2$  powders at impact velocities of 1.5–2 km/s using a single capsule geometry, with and without the addition of copper powder to vary the shock-loading pressure (calculated to be 22–58 GPa) and temperature (calculated to be up to 3250 °C) in the sample. No evidence of shock-induced decomposition was observed in these recovery experiments performed on the  $\text{Ti}_3\text{SiC}_2$  powders. © 2003 American Institute of Physics. [DOI: 10.1063/1.1573345]

## I. INTRODUCTION

Titanium–silicon ternary carbide ( $\text{Ti}_3\text{SiC}_2$ ) is a unique material because it maintains high-temperature properties and wear resistance typical of ceramics while also demonstrating metal-like properties including high electrical and thermal conductivity, and easy machinability.<sup>1</sup> It is an elastically stiff but soft (low hardness) material. While in most materials hardness typically scales with the elastic modulus,  $\text{Ti}_3\text{SiC}_2$  shows an anomalous behavior. It is very incompressible and it has a bulk modulus (206 GPa)<sup>2</sup> similar to that of TiC (~220 GPa). Its elastic modulus (320 GPa)<sup>1</sup> and shear modulus (133 GPa)<sup>2</sup> are similar to those of metallic molybdenum ( $E=318$  GPa and  $\mu=122$  GPa). On the other hand, its hardness is comparable to that of quenched high carbon steels. The unique properties of this ternary ceramic are attributed to its layered structure, which consists of TiC octahedra separated by layers of silicon atoms. The incompressibility and the metal-like deformation response of this ternary ceramic make it a potentially interesting damage tolerant armor material.

Although the structural characteristics and mechanical properties of this material have been extensively studied, its dynamic mechanical behavior and high pressure phase stability have not been characterized. The static high pressure compressibility properties were measured by Onodera *et al.*<sup>2</sup>

They found a continuous pressure–volume compressibility behavior, indicating no phase transformation or decomposition during static application of pressure up to 60 GPa at room temperature. This article will present results of dynamic high pressure compressibility and phase stability behavior determined from Hugoniot measurements performed at pressures up to 120 GPa and recovery experiments followed by postmortem microstructural analysis.

## II. EXPERIMENTAL PROCEDURE

The  $\text{Ti}_3\text{SiC}_2$  samples used in the present work were synthesized using the method described in Ref. 1. They were obtained from 3-One-2, LLC, in the form of 62.5-mm-diam by 5-mm-thick disks, from which 10 mm × 12 mm rectangles of 2.75 mm thickness were electro-discharged machined for performing the Hugoniot measurements. An x-ray diffraction (XRD) pattern of the starting material is shown in Fig. 1(a), with the  $\text{Ti}_3\text{SiC}_2$  peaks identified by their  $hkl$  values. A trace of TiC phase was also observed, as indicated in the figure. To prepare the powder used in the recovery experiments, solid  $\text{Ti}_3\text{SiC}_2$  compacts were ball milled using a Spex mill. XRD analysis of the ball-milled powder showed extensive peak broadening as illustrated in Fig. 1(b), but no obvious pickup of impurity or change in composition.

Hugoniot experiments for equation of state measurements were conducted using a two-stage light gas gun at the National Institute for Materials Science (NIMS), in Tsukuba, Japan. The experimental setup<sup>3</sup> shown in Fig. 2 was used to

<sup>a)</sup> Author to whom correspondence should be addressed; electronic mail: naresh.thadhani@mse.gatech.edu

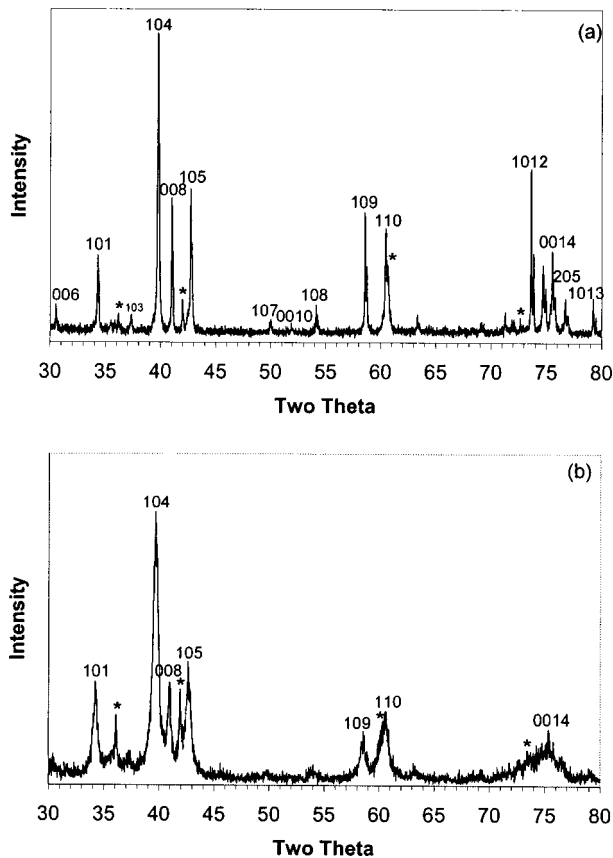


FIG. 1. X-ray diffraction patterns of: (a) as-received (starting) material used for time-resolved Hugoniot measurements and (b) as-ground powder used for shock recovery experiments, with the  $\text{Ti}_3\text{SiC}_2$  peaks identified by their  $hkl$  values and trace of TiC phase denoted by (\*) symbol.

measure the shock velocity based on time of travel through the sample thickness, given by the extinction times of mirrors  $M1/M4$  and  $M2/M3$ . The particle velocity was determined from the free surface velocity, which was measured using the inclined mirror method. Signals from mirrors  $M1$ ,

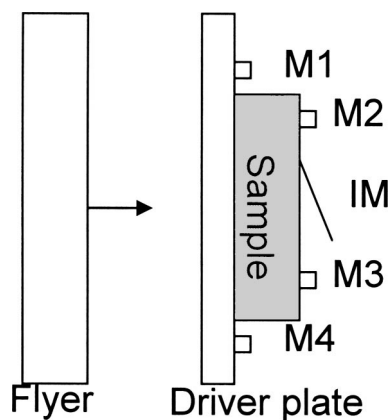


FIG. 2. Schematic of the inclined mirror method of measuring shock and free surface velocity. The inclined mirror is indicated by IM, and the flat mirrors are indicated by  $M1-M4$ . Extinction of the reflectivity of mirrors  $M1$  and  $M4$  indicate the arrival time of the shock wave at the front surface of the sample. Extinction of the reflectivity of  $M2$  and  $M3$  indicates the arrival of the shock wave at the back surface of the sample. The inclined mirror gives a profile of the free surface velocity with time (Ref. 3).

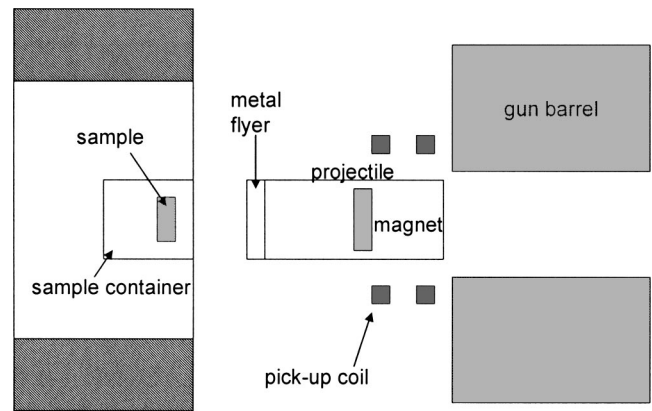


FIG. 3. Schematic of recovery experiment using NIMS propellant gun. The powder sample in a metal container is used for the target. The projectile consists of a metal flyer plate and a plastic sabot with a magnet embedded in the rear surface. The magnet is used to measure the projectile impact velocity (Ref. 4).

$M2$ ,  $M3$ ,  $M4$ , and the inclined mirror were recorded using a streak camera. Values of the particle velocity were also calculated using the impedance matching method and the measured impact velocity.

The shock recovery experiments were conducted using the NIMS propellant gun. As shown in the schematic of the impact setup in Fig. 3,<sup>4</sup> the powder sample is placed in a metal container, which is used as the target. The projectile consists of a metal flyer plate mounted on a plastic sabot with a magnet embedded in it, to measure the projectile impact velocity.<sup>4</sup>

### III. RESULTS AND DISCUSSION

Hugoniot equation of state experiments involved measurements of shock and particle velocities recorded on a streak camera. The numerical values of the measured parameters [shock ( $U_s$ ) and particle velocity ( $U_p$ )] for experiments performed at different impact velocities are given in Table I. The particle velocity calculated from the impedance matching method is also listed. It should be noted that the calculated particle velocities are lower than those obtained from free surface velocity measurements. The difference in the measured and calculated particle velocities is attributed to the presence of tilt in the experiment. While the streak camera records of free surface velocity measurements show interesting features (to be discussed later), only the calculated particle velocity values are used for subsequent data analysis. Values of the shock pressure and relative volume ( $V/V_0$ ) calculated using jump conditions and the measured  $U_s$  and calculated  $U_p$  values are also listed in Table I.

The shock temperature was also calculated from the Hugoniot experiments based on the following equation:<sup>5</sup>

$$T_H = T_0 \exp \left[ \left( \frac{\gamma_0}{V_0} \right) (V_0 - V) \right] + \frac{P_H (V_0 - V)}{2C_V} + \frac{1}{C_V} \int_{V_0}^V P_S dV - \frac{\Delta E_{tr}}{C_V}, \quad (1)$$

TABLE I. Summary of results from equation of state experiments.

Shot No.	Impact geometry	Velocity (km/s)	Measured $U_S$ (km/s) <sup>a</sup>	Measured $U_P$ (km/s) <sup>b</sup>	Calculated $U_P$ (km/s) <sup>c</sup>	Calculated pressure (GPa)	Calculated $V/V_0$	Calculated temperature (K)
T-177	Aluminum flyer stainless steel driver	3.61	8.53±0.1	1.88	1.27	49	0.85	607
T-175	Stainless steel flyer and driver	4.02	9.31±0.2	3.18	2.31	96	0.75	1468
T-176 (two slopes)	Stainless steel flyer and driver	4.87	9.67±0.2	2.31	2.81	122	0.71	2169
			9.21±0.2	3.67	2.86	118	0.69	2052

<sup>a</sup>Shock velocity measured based on the extinction times of mirrors  $M1/M4$  and  $M2/M3$  in Fig. 1(a).

<sup>b</sup>Particle velocity determined from the free surface velocity, which was measured using the inclined mirror method.

<sup>c</sup>Particle velocity calculated from the impedance matching method.

where  $T_H$  is the shock temperature,  $T_0$  is a reference temperature,  $\gamma_0$  is the Mie–Grüneisen coefficient,  $P_H$  is the shock pressure,  $V_0$  is the specific reference volume,  $C_V$  is the constant volume heat capacity, and  $P_S$  is given by the Birch–Murnaghan equation

$$P_S = \frac{3K_0}{2} \left[ \left( \frac{V_0}{V} \right)^{7/3} - \left( \frac{V_0}{V} \right)^{5/3} \right] \times \left[ 1 + 3 \left( \frac{K'_0}{4} - 1 \right) \left( \left( \frac{V_0}{V} \right)^{2/3} - 1 \right) \right], \quad (2)$$

where  $K_0$  is the bulk modulus and  $K'_0$  is the pressure derivative of the bulk modulus. The values of  $K_0$  and  $K'_0$  were taken to be 206 GPa and 4, respectively, from Onodera’s results.<sup>2</sup> The values of  $C_0$  and  $S$  were obtained from the  $U_S - U_P$  linear relationship calculated using Onodera’s data, de-

scribed later. The value of the Grüneisen constant,  $\gamma_0$  was approximated to be equal to  $2S - 1$ . The integral of  $P_S$  in the above equations was evaluated numerically. The calculated shock temperatures determined from the Hugoniot experiments are presented in Table I.

The streak records of the three inclined mirror experiments are shown in Figs. 4(a)–4(c). Figure 4(a) shows a clear record of free surface velocity with a single slope. Figures 4(b) and 4(c) show blurred edges in the records of the free surface velocity. The blurred edges may be indicative of the presence of several phases having been formed due to shock-induced structural or chemical changes. The higher pressure record [Fig. 4(c)] shows a distinct change in slope illustrating an obvious change in the state of the material as a result of a shock-induced transformation.

Figure 5 shows the static pressure–volume compressibility data of Onodera *et al.*<sup>2</sup> extended to higher pressures by curve fitting the data. The pressure–volume data obtained from the measured shock velocity and calculated particle velocity in the present experiments (listed in Table I) are also shown in Fig. 5. It can be seen that while the 49 GPa data point falls on the same curve as that of the low pressure (static) data of Onodera *et al.*,<sup>2</sup> data obtained from the present experiments at two higher pressures show deviation indicating possible phase change to an increased compressibility state.

The static high pressure data from Onodera *et al.* was also converted to shock and particle velocity data using jump

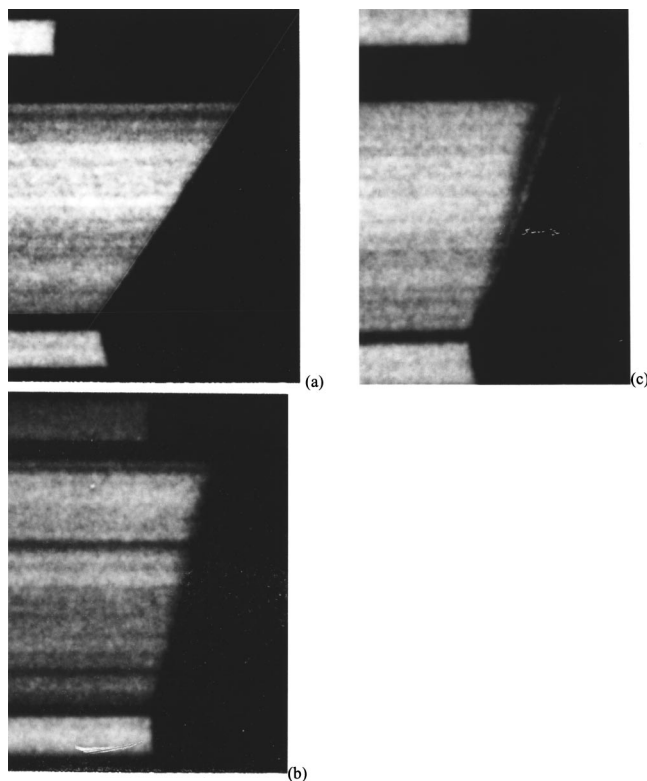


FIG. 4. (a) Streak record from experiment T-177; (b) streak record from experiment T-175; and (c) streak record from experiment T-176.

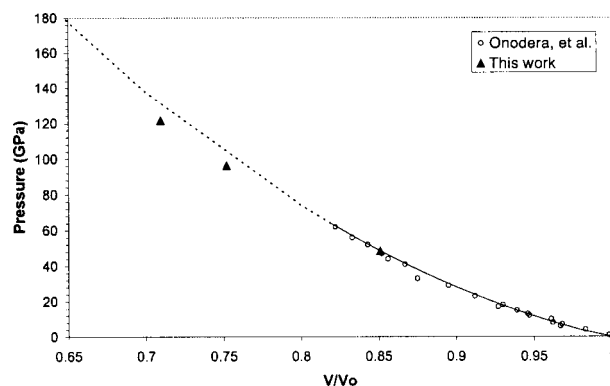


FIG. 5. Pressure vs volume plot with Onodera *et al.* (Ref. 2) data and data from the three equation of state experiments.

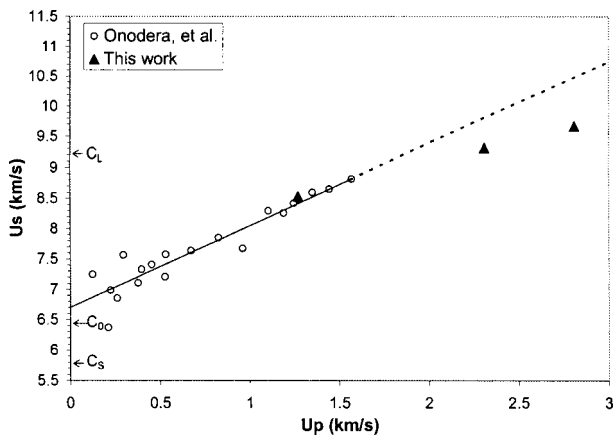


FIG. 6. Particle velocity vs shock velocity with Onodera's data and data from the Tsukuba experiments. Onodera's data was converted from the reported pressure–volume data using  $U_s = C_0 V_0 / V_0 - S(V_0 - V_1)$  and  $U_p = (C_0/2S)[\sqrt{1 + (4S/\rho_0 C_0^2)P} - 1]$ . The particle velocities in the Tsukuba experiments were calculated from the measured shock velocity using an impedance matching method.

conditions. The linear fit to the data yielded the shock velocity–particle velocity relationship given by the following:

$$U_s = 6.70 + 1.34 * U_p. \quad (3)$$

Figure 6 shows the  $U_s - U_p$  data obtained from the current shock experiments at high pressures plotted along with the static high pressure data of Onodera *et al.*<sup>2</sup> Values of longitudinal, shear, and bulk sound speed of the  $\text{Ti}_3\text{SiC}_2$  samples measured using an ultrasound technique are also presented. It can be seen that the low pressure (49 GPa) data point from the present work falls on the same  $U_s - U_p$  linear trend extrapolating on Onodera's data, while the higher pressure data points show a deviation from linearity to an increased compressibility state. The deviation is again indicative of a possible phase change from a lower to higher density state, occurring in the range of 50–75 GPa. Evidence of phase change is further confirmed by the blurred edge of the inclined mirror record in experiment T-175 (at  $\sim 96$  GPa), shown in Fig. 4(b), and the presence of two distinct slopes in the streak record of experiment T-176 (at  $\sim 122$  GPa), shown in Fig. 4(c).

Shock compression recovery experiments were also performed on  $\text{Ti}_3\text{SiC}_2$  using the fixture illustrated in Fig. 3. A summary of the recovery experiments conducted is given in Table II. One experiment (Shot No. 926) contained pure  $\text{Ti}_3\text{SiC}_2$  powder, and two experiments (Shot Nos. 927 and 930) contained  $\text{Ti}_3\text{SiC}_2$  powder mixed with copper powder.

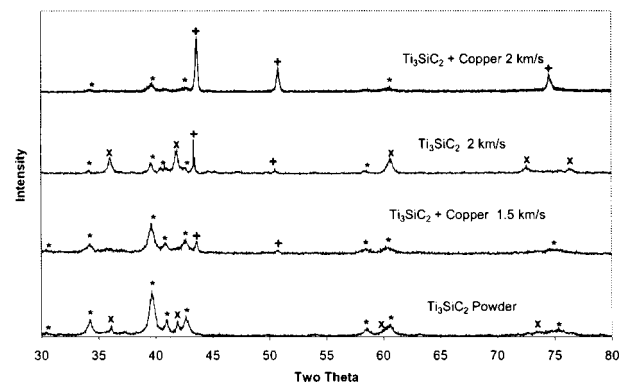


FIG. 7. X-ray diffraction patterns of recovery experiments where an (\*) indicates the  $\text{Ti}_3\text{SiC}_2$  peaks, an (x) indicates TiC peaks, and (+) indicates steel contamination.

The copper powder was used to increase the maximum peak pressure and correspondingly the shock energy and bulk temperature generated during shock compression. Shock compression of the powders in solid-density containers, can be dominated by two-dimensional wave propagation effects. Hence, Autodyn-2D,<sup>6</sup> a wave propagation code, was used to compute the peak pressures and bulk temperatures generated in the 18-mm-diam by 1-mm-thick region of the powder compacts. The range of equilibrated peak shock pressures and maximum bulk shock temperatures at the impact and nonimpact surfaces calculated with Autodyn-2D for experiments 930, 926, and 927 are given in Table II. It can be seen that the equilibrated peak shock pressure is only slightly higher in the  $\text{Ti}_3\text{SiC}_2 + \text{copper}$  powder experiment (No. 927) compared to that in the  $\text{Ti}_3\text{SiC}_2$  experiment (No. 926) both of which were conducted at 2 km/s. However, the corresponding maximum bulk shock temperature in the experiment with the copper powder (No. 927), in contrast to that in just  $\text{Ti}_3\text{SiC}_2$  (No. 926), is much higher due to the larger internal (strain) energy and lower specific heat associated with the addition of copper. Likewise, the highest peak pressure in the recovery experiments is in the range of the low pressure Hugoniot experiments, however the temperature in these recovery experiments is higher due to the higher compression associated with powders (72%–91% dense).

The x-ray diffraction patterns of the recovered shock compressed samples and the starting powder are shown in Fig. 7.  $\text{Ti}_3\text{SiC}_2$  is indicated by the symbol (\*), (x) indicates TiC peaks, and (+) indicates peaks corresponding to steel contamination, due to interaction with the container material. It can be seen that while the amount of the contamination phase increases with increasing pressure and temperature

TABLE II. Summary of recovery experiments.

Shot No.	Powder	Initial density (% TMD)	Projectile velocity (km/s)	Peak pressure (GPa)		Maximum bulk temperature (°C)	
				Impact	Nonimpact	Impact	Nonimpact
930	93% Cu + $\text{Ti}_3\text{SiC}_2$	91	1.49	22–27	31–43	1360–1430	1810–2160
926	$\text{Ti}_3\text{SiC}_2$	72	1.96	46–47	47–49	1090–1210	1330–1400
927	93% Cu + $\text{Ti}_3\text{SiC}_2$	81	1.97	43–45	46–58	2380–2440	2940–3250

(maximum in the sample containing Cu mixed with  $\text{Ti}_3\text{SiC}_2$  powder), the  $\text{Ti}_3\text{SiC}_2$  phase itself remains present in all of the recovered shock-compressed samples without undergoing any decomposition or phase change under the imposed shock-loading conditions.

While the powder recovery experiments show no evidence of shock-induced decomposition of  $\text{Ti}_3\text{SiC}_2$ , time-resolved measurements performed to determine the pressure-versus-volume compressibility and Hugoniot equation of state show clear evidence of a pressure-induced phase transformation to a high-density state at pressures exceeding 46 GPa. The streak camera records of experiments performed at 96 and 122 GPa, show distinct features (blurred edges and change in slope) indicative of events corresponding to a phase change. Likewise, the pressure-versus-volume and shock-velocity versus particle velocity plots show obvious deviations from the trends at lower pressure, thereby providing clear evidence of the transformation of  $\text{Ti}_3\text{SiC}_2$  to a more condensed phase(s).

It should be noted that the thermal decomposition of  $\text{Ti}_3\text{SiC}_2$  at ambient pressure has been reported to be greater than 2300 °C, with the decomposition products believed to be  $\text{Ti}_3\text{C}_2$  and silicon.<sup>7,8</sup> The calculated bulk temperature produced during shock compression in the experiments conducted in the present work is greater than the decomposition temperature. However, the time at temperature is not sufficient for diffusion-type reactions to occur. The phase change observed in Hugoniot experiments is an effect of pressure-induced phase transformation. The lack of pressure-induced phase change or thermally initiated decomposition in recovery experiments is not an unexpected result under the imposed shock loading conditions.

#### IV. CONCLUSIONS

Time-resolved measurements of pressure–volume compressibility and Hugoniot equation of state were conducted on titanium–silicon carbide ( $\text{Ti}_3\text{SiC}_2$ ) samples in the pressure range of 50–120 GPa. At pressures around 90–120 GPa,  $\text{Ti}_3\text{SiC}_2$  was found to transform to a more condensed state. Shock-recovery experiments were also performed on  $\text{Ti}_3\text{SiC}_2$  powders, with and without the addition of copper powder to vary the shock-loading pressure and temperature history in the sample. No evidence of shock-induced decomposition was observed in these experiments.

#### ACKNOWLEDGMENTS

This work was accomplished while Jennifer Jordan was participating in the Summer Program for Graduate Students in Japan sponsored by the National Science Foundation. Funding for research was provided in part by the National Institute for Materials Science, Tsukuba, Japan, and ARO Grant Nos. DAAG55-98-1-0454 and DAAG55-98-1-0161.

- <sup>1</sup>M. Barsoum and T. El-Raghy, *J. Am. Ceram. Soc.* **79**, 1953 (1996).
- <sup>2</sup>A. Onodera, H. Hirano, T. Yuasa, N. F. Guo, and Y. Miyamoto, in *Science and Technology of High Pressure*, edited by M. H. Manghnani, W. J. Nellis, and M. F. Nicol (Universities Press, India, 2000).
- <sup>3</sup>T. Sekine, S. Tashiro, T. Kobayashi, and T. Matsumura, in *Shock Compression of Condensed Matter — 1995*, edited by W. C. Tao (AIP, Woodbury, NY, 1996), pp. 1201–1204.
- <sup>4</sup>T. Sekine, *Eur. J. Solid State Inorg. Chem.* **34**, 823 (1997).
- <sup>5</sup>S. C. Gupta, S. G. Love, and T. J. Ahrens, *Earth Planet. Sci. Lett.* **201**, 1 (2002).
- <sup>6</sup>Autodyn-2D, Century Dynamics Incorporated, Oakland, CA, 1995.
- <sup>7</sup>M. W. Barsoum, *Prog. Solid State Chem.* **28**, 201 (2000).
- <sup>8</sup>Y. Du, J. C. Schuster, H. Seifert, and F. Aldinger, *J. Am. Ceram. Soc.* **83**, 197 (2000).